Chalcogenide Letters Vol. 12, No. 4, April 2015, p. 161 - 172

STRUCTURAL OPTICAL AND ELECTRICAL PROPERTIES OF $Zn_xCu_{1-x}S$ NANOPARTICLE SYSTEM

R. SHEELA CHRISTY[a*], J.T. THANKA KUMARAN[a], C. BANSAL[b], M. BRIGHTSON[c]
[a]*Research centre, Department of Physics, N.M.C.College, Marthandam, Tamil Nadu, India*
[b]*School of Physics, University of Hyderabad, India*
[c]*Department of Physics, St.Jude'scollege,Thoothoor, Tamil Nadu, India*

$Zn_xCu_{1-x}S$, x=1, .8, .6, .4 and .2 nanoparticles were synthesized by solvothermal method. The as-synthesized nanoparticles were characterized by X ray diffraction to study the crystal structure and size. The structure of $Zn_xCu_{1-x}S$ nanoparticles depends on the value of x. Room-temperature photoluminescence (PL) measurements of the system showed two peaks, one around 475nm and another around 515 nm. The D.C electrical resistance was measured in the temperature range 310K-485K. As copper sulfide nanoparticles shows a phase transition around 470K, the effect of this transition is seen in the resistance measurements and in the UV-VIS spectra of most of the samples in the system. After heavy oscillation $Zn_{.6}Cu_{.4}S$ nanoparticles shows a drastic jump in resistance from $10^8\Omega$ to $10^3\Omega$ at 470K. The band gap energies calculated from resistance measurements agree with the band gaps obtained from UV-VIS spectra.

(Received January 20, 2015; Accepted April 7, 2015)

Keywords: Nanoparticles; Solvothermal method; Structural; Band gap energy

1. Introduction

ZnS is an important direct band gap semiconductor. It has a band gap energy of 3.6 eV[1], displays a high refractive index[2] and a high transmittance in the visible range [3,4] making this material a strong candidate for use in optoelectronic devices. ZnS not only exhibits photoluminescence [5], but also acoustoluminescence [6], triboluminescence [7], electroluminescence [8] and thermoluminescence [9] lending the material to promising applications in flat panel display sensors and lasers.

CuS is also an important semiconductor that has a direct band gap of 2.5eV for bulk hexagonal wurtzite structure [10]. Copper sulfides can find applications in photo thermal conversion, solar cell devices, coatings for microwave shields and solar control [11]. Resistance measurements on copper sulfide nanoparticles show a phase transition around 470K [12].

$Zn_xCu_{1-x}S$ nanoparticle system can have the applications of both ZnS and CuS. Hong E and Kim fabricated ZnS-CuS nanoparticle compound and used it for solar hydrogen production [13]. Shifu and Mingsong synthesized ZnS-CuS nanoparticles by precipitation method and the photocatalytic activity was evaluated [14]. In the present work $Zn_xCu_{1-x}S$, x=1, .8, .6, .4 and .2 nanoparticles were synthesized by solvothermal method. Their optical properties were studied using UV-VIS spectra and PL spectra and electrical properties using resistance measurements. The band gap energies obtained from resistance measurements are compared with the band gap energies from UV-VIS spectra.

*Corresponding author: sheelachristy64@yahoo.com

2. Experimental details

2.1 Synthesis of $Zn_xCu_{1-x}S$ nanoparticles by solvothermal method

Analytical Reagent (A.R) grade Zinc acetate, copper (11) acetate and thiourea along with ethylene glycol were used for the preparation of nanocrystals $Zn_xCu_{1-x}S$. Zinc acetate and copper (11) acetate taken together in the required composition and thiourea in 1:3 molecular ratio were mixed and dissolved in 50 ml of ethylene glycol and kept in a domestic microwave oven. The amount of precursor materials taken are given in Table 1.

Table 1

Expected composition	Amount of precursors(in gram)		
	Zinc acetate	copper(11) acetate	Thiourea
ZnS	10.98	---	11.42
$Zn_{.8}Cu_{.2}S$	8.78	2	11.42
$Zn_{.6}Cu_{.4}S$	6.59	3.99	11.42
$Zn_{.4}Cu_{.6}S$	4.39	5.99	11.42
$Zn_{.2}Cu_{.8}S$	2.2	7.99	11.42

Microwave irradiation was carried out until the solvent gets evaporated. The colloidal precipitate obtained was cooled to room temperature naturally and washed with doubly distilled water and then with acetone to remove the organic impurities if any. The samples were then filtered and dried in atmospheric air and collected as the yield. They were finally annealed at about 50^0 C for one hour to get phase pure nanoparticles.

2.2 Instrumentation

X-ray diffraction (XRD) patterns of the samples were recorded on a Philips model PW-1830 X-ray diffractometer with Co Kα radiation of wavelength 1.788A^0 in the range of scanning angles 10^0-90^0. The scanning electron microscope was used to study the surface morphology. Topographic image of ZnS was recorded with a multimode atomic force microscope. Optical absorption spectra of the samples were recorded on UV-VIS spectrometer in the wavelength range 200-900nm. Photoluminescence (PL) spectra were recorded using Luminescence Spectrometer (Perkin Elmer LS45). The materials were pelletized by applying high pressure 10 tons. The resulting pellet is a compressed collection of nanoparticles. The resistances of the pellet form of the samples were measured by the four probe technique.

3. Results and discussion

3.1 Structural studies

Fig (1a) shows the XRD pattern of ZnS nanoparticles synthesized by solvothermal method. Broad and diffused pattern of XRD lines are indicative of the small size of the ZnS nanoparticles and this pattern confirmed the formation of cubic ZnS, which matches with the standard JCPDS file (5-0566). A c++ program was developed to fit the peaks of the XRD patterns to gaussian and from the width of the gaussian the particle sizes were calculated using Scherrer method [15]. Fig (1b) shows the Gaussian fitted (1 1 1) peak of the zinc sulfide nanoparticles. The particle size calculated is 2nm. The SEM image of the powdered sample (fig 1c) shows the uniform distribution of ZnS nanoparticles. AFM image (fig1d) confirms the nano size of the particles.

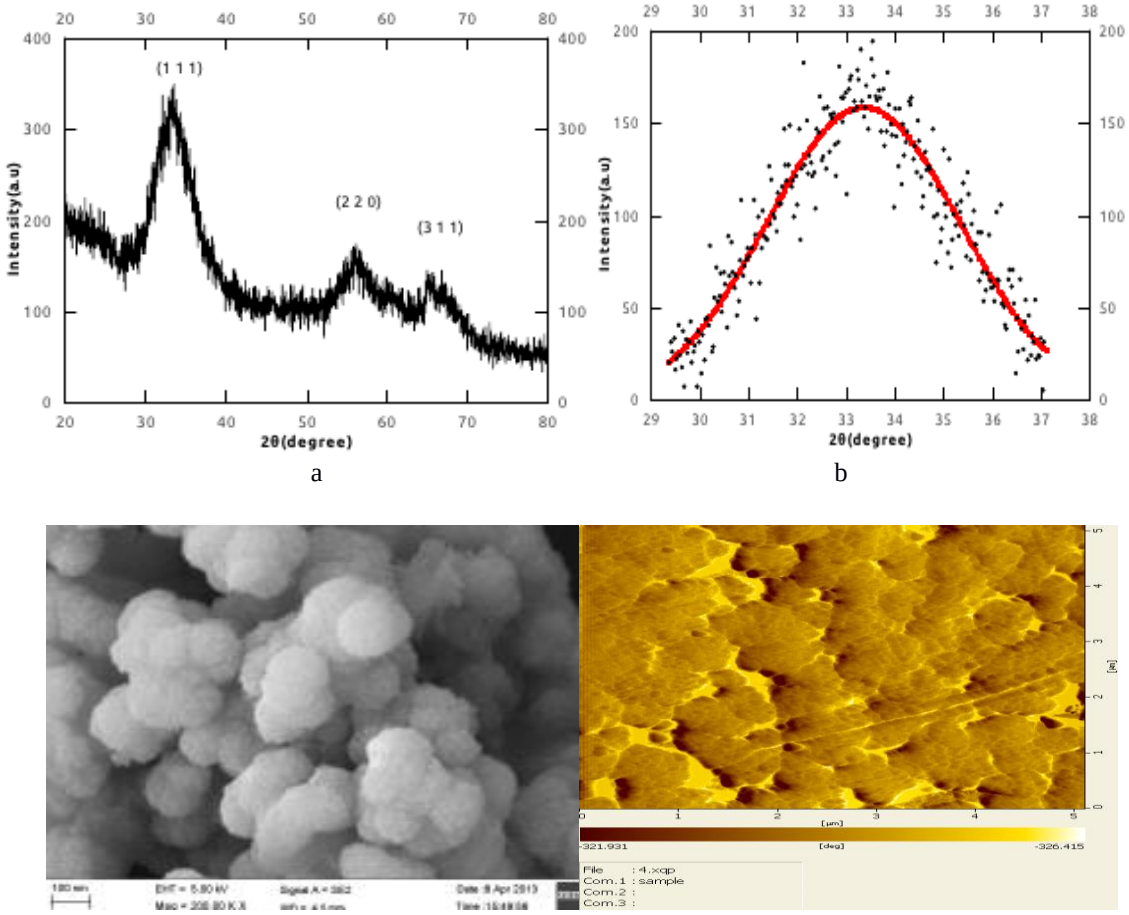

Fig 1. (a) XRD pattern of zinc sulfide nanoparticles,(b) Gaussian fitted (1 1 1) peak of the ZnS nanoparticles. (c) SEM image of zinc sulfide nanoparticles, (d) AFMimage of zinc sulfide nanoparticles.

Fig (2a) shows the XRD pattern of $Zn_{.8}Cu_{.2}S$ nanoparticles synthesized by solvothermal method. The XRD pattern exhibits prominent broad peaks at 33.4^0, 57.4^0 and 68^0 which could be indexed to scattering from (1 1 1), (2 2 0), (3 1 1) planes of cubic phase. Broadening of the peaks indicates the nano crystalline nature of the material and the crystalline size is 2.6nm.

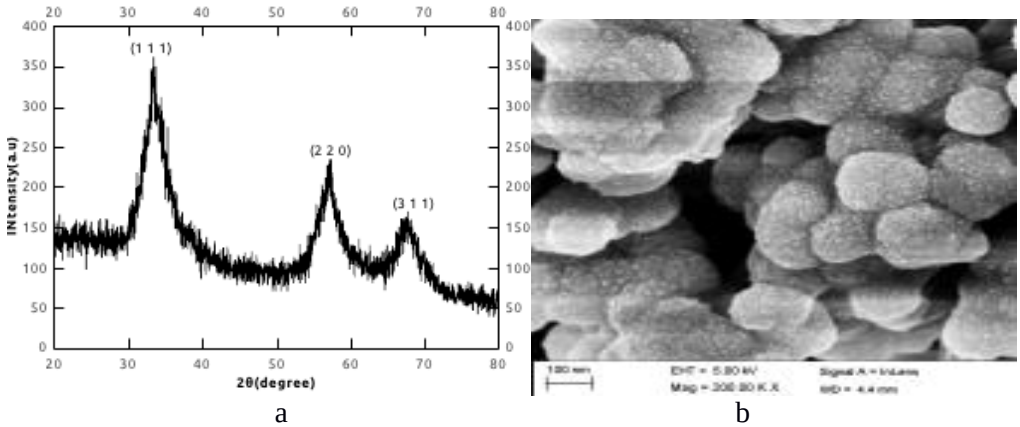

Fig. 2.a) XRD pattern of $Zn_{.8}Cu_{.2}S$ nanoparticles, b) SEM image of $Zn_{.8}Cu_{.2}S$ nanoparticles

XRD pattern of $Zn_{.6}Cu_{.4}S$ nanoparticles (fig 3a) can be indexed with hexagonal structure with lattice parameters a=3.8 Å and c=17 Å .The particle size calculated is 10.8 nm. Now the structure shifts from cubic (structure of ZnS) to hexagonal (structure of CuS).

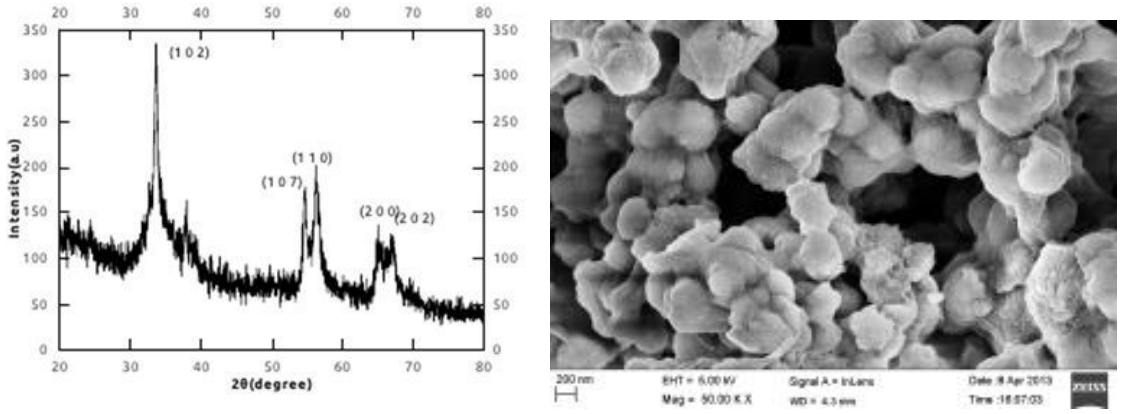

a b

Fig 3.a) XRD pattern of $Zn_{.6}Cu_{.4}S$ nanoparticles, b) SEM image of $Zn_{.6}Cu_{.4}S$ nanoparticles .

XRD pattern of $Zn_{.4}Cu_{.6}S$ nanoparticles (fig 4a) can be indexed with hexagonal structure with lattice parameters a=3.85Å and c=16Å, where the particle size calculated is 20nm.

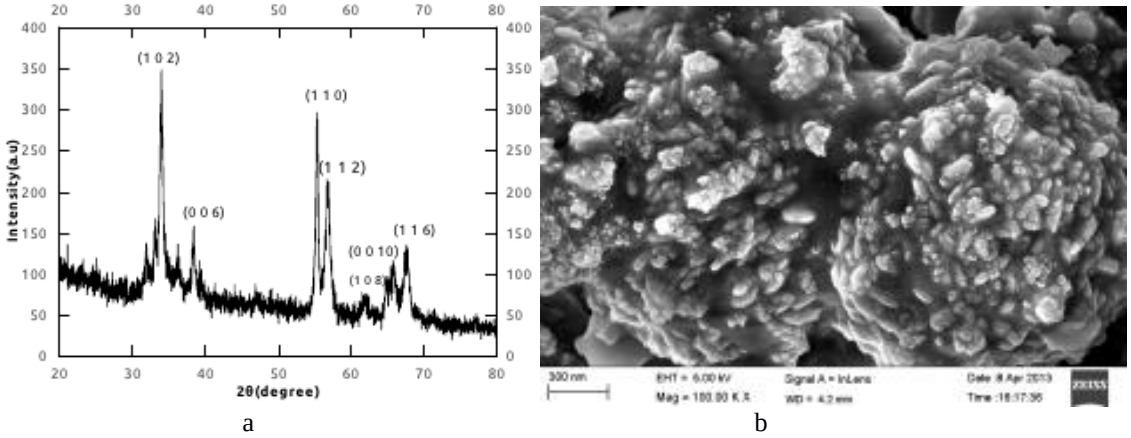

a b

Fig 4.a) XRD pattern of $Zn_{.4}Cu_{.6}S$ nanoparticles, b) SEM image of $Zn_{.4}Cu_{.6}S$ nanoparticles.

XRD pattern of $Zn._2Cu_{.8}S$ nanoparticles (fig 5a)synthesized can also be indexed with hexagonal structure with lattice parameters a=3.9 Å and c=16.5 Å. The particle size calculated is 21 nm.

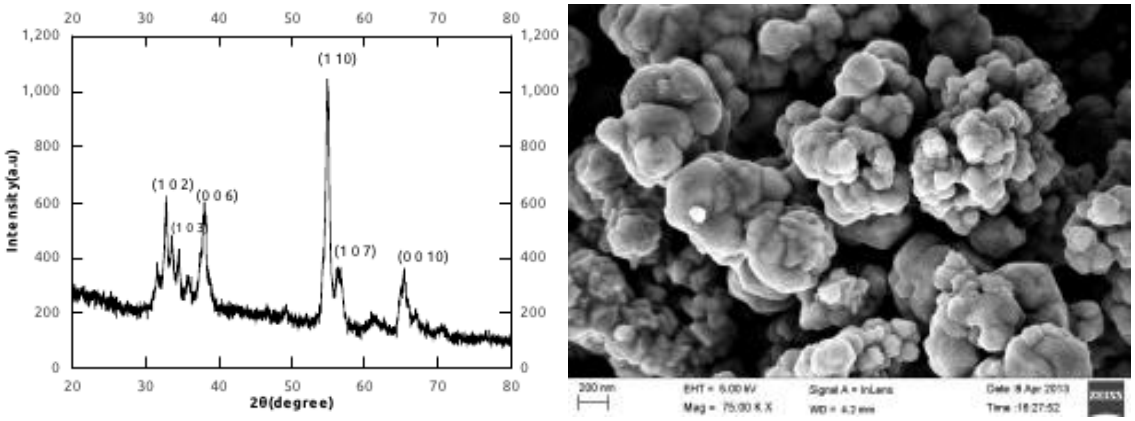

Fig 5.a) XRD pattern of $Zn_{.2}Cu_{.8}S$ nanoparticles, b) SEM image of $Zn_{.2}Cu_{.8}S$ nanoparticles.

SEM image of all the above samples (figures 2b, 3b, 4b, 5b) show the uniform distribution of nanoparticles and also confirm the nano size of the particles. The structure, lattice parameters and particle size for different composition are tabulated in table 2. The particle size increases as the content of copper sulfide is increased.

Table 2

Composition	Structure	Lattice Parameters Å	Size Nm
ZnS	Cubic	a=5.36	2
$Zn_{.8}Cu_{.2}S$	Cubic	a=5.26	2.6
$Zn_{.6}Cu_{.4}S$	Hexagonal	a=3.8, c=17	10.8
$Zn_{.4}Cu_{.6}S$	Hexagonal	a=3.85, c=16	20
$Zn_{.2}Cu_{.8}S$	Hexagonal	a=3.9, c=16.5	21
CuS(reported)	Hexagonal	a=3.8, c=16.4	

3.2 Optical studies

Fig (6a) shows the optical absorption spectrum of ZnS nanoparticles. There is only one absorption band with edge around 350nm (3.5eV) which is in close agreement with the value of the bulk [1]. Fig (6b) shows the PL emission spectrum of the zinc sulfide nanoparticles. There is an emission band (460nm-490nm) with peak around 475nm and another one having peak around 515 nm exist. Peak in between 470 nm and 520 nm was also observed by Nada K Abbas and Khalid T [16]. PL spectrum with peak at 516nm was also observed by H.V.Chung and P.T.Huy for ZnS nanostructures synthesized using thermal evaporation technique [17].

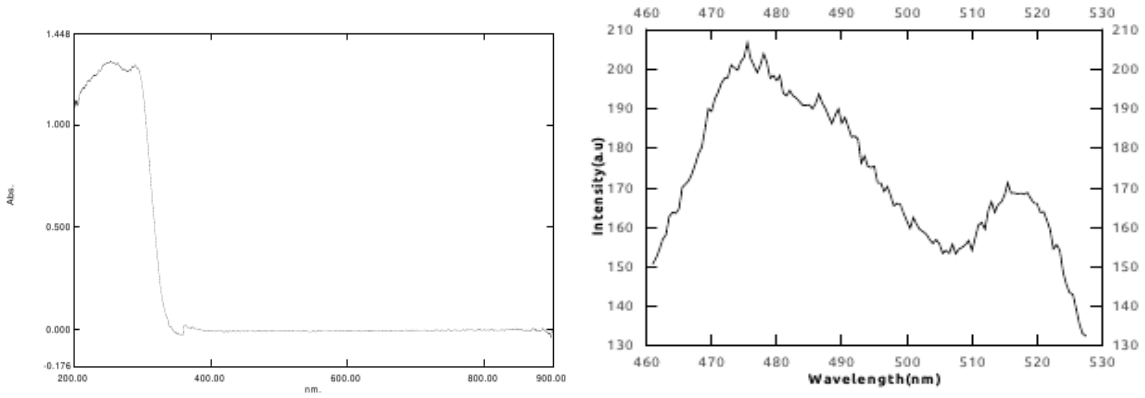

a b

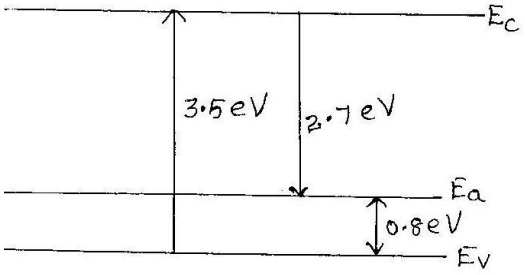

c

Fig6.a) UV absorption spectrum of ZnS nanoparticles, b) PL emission spectrum of ZnS nanoparticles, c) Energy level diagram for absorption and emission of ZnS nanoparticles

So it start absorption at 350nm (3.5 eV) and start emission from 460nm (2.7eV)) . So there exists an energy level with energy around 0.8 eV above the valance band. Fig (6c) shows the emission absorption energy level diagram.

Fig (7a) shows the optical absorption spectrum of $Zn_{.8}Cu_{.2}S$ nanoparticles. There is only one absorption band with edge around 400nm. Fig (7b) shows the PL emission spectrum of the zinc sulfide nanoparticles. The peaks are observed around 475nm and 515nm. Intensity of the first peak is reduced .

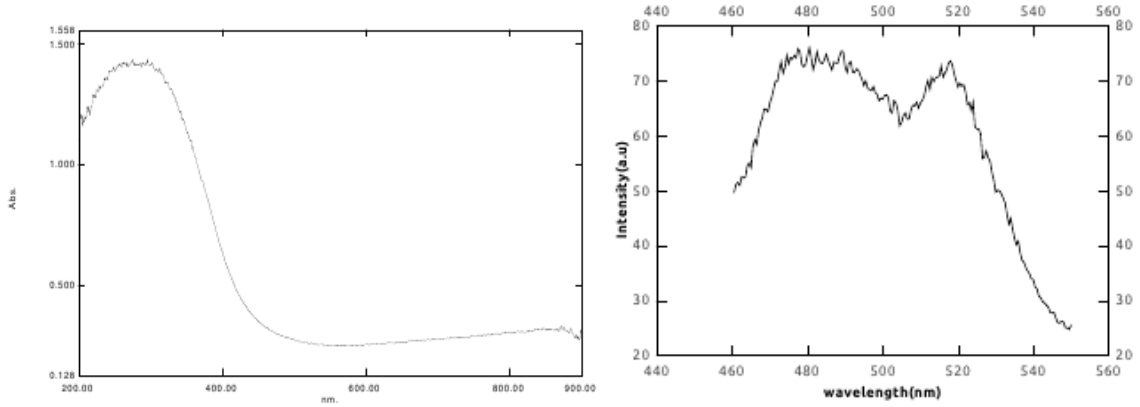

Fig.7.a) UV absorption spectrum of Zn.8Cu.2S nanoparticles, b)PL emission spectrum of Zn.8Cu.2Snanoparticles.

Optical absorption spectrum of $Zn_{.6}Cu_{.4}S$ nanoparticles (fig 8a) shows one absorption band with edge around 560nm (2.3eV) and another with edge around 900 nm (1.4eV). Fig (8b) shows

the PL emission spectrum of the $Zn_{.6}Cu_{.4}S$ nanoparticles. Peaks are observed around 490nm and 515nm. Intensity of the first peak is further reduced and shifted as the composition of copper sulfide increased.

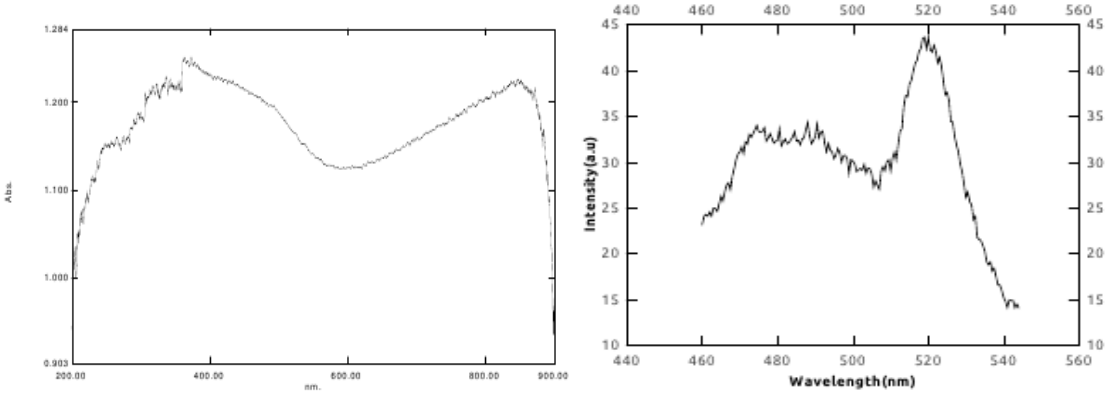

Fig 8.a) UV absorption spectrum of Zn.6Cu.4S nanoparticles, 8b) PL emission spectrum of $Zn_{.6}Cu_{.4}S$ nanoparticles.

Fig (9a) shows the optical absorption spectrum of $Zn_{.4}Cu_{.6}S$ nanoparticles. There is one absorption band with edge around 590nm (2.0eV) and another with edge around 900 nm (1.4eV). Fig (9b) shows the PL emission spectra of the $Zn_{.4}Cu_{.6}S$ nanoparticles. The peaks are observed around 490nm and 520nm. Intensity of the first peak is further reduced and the second peak is slightly shifted as reported by W.Q.Peng and G.W.Cong [18].

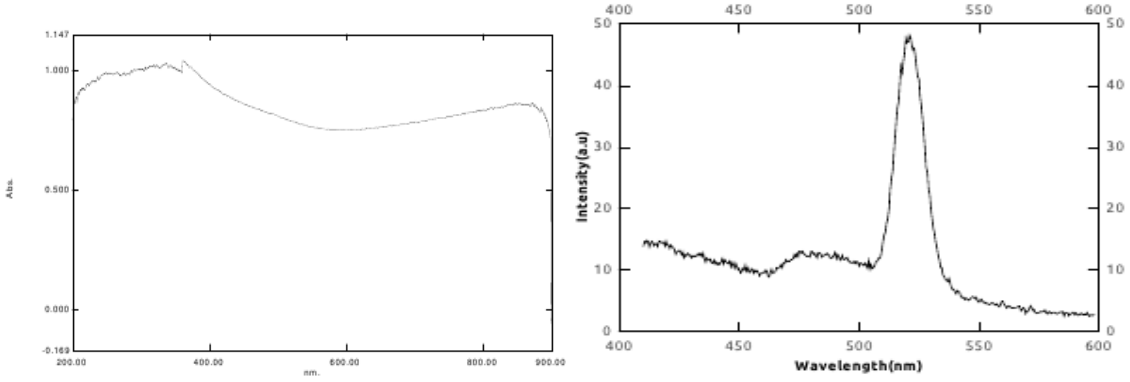

a b

Fig 9.a) UV absorption spectrum of Zn.4Cu.6S nanoparticles, b) PL emission spectrum of $Zn_{.4}Cu_{.6}S$ nanoparticles.

Fig (10a) shows the optical absorption spectrum of $Zn_{.2}Cu_{.8}S$ nanoparticles. There exists an absorption band from 400nm to 900 nm. Fig (10b) shows the PL emission spectrum of the $Zn_{.2}Cu_{.8}S$ nanoparticles. There is only one peak observed around 520nm.

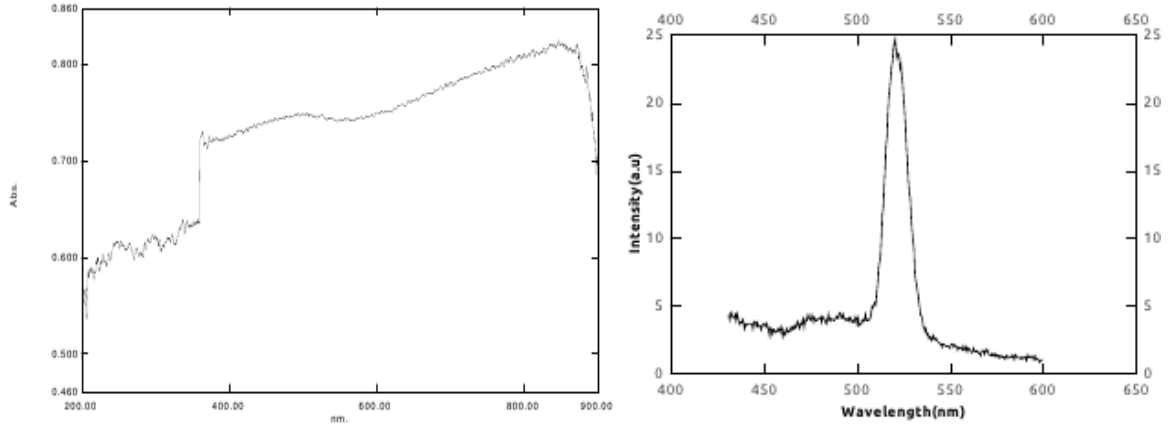

Fig10a)UV absorption spectrum of Zn.4Cu.6S nanoparticles, b)PL mission spectrum of $Zn_{.4}Cu_{.6}S$ nanoparticles.

Absorption spectrum with single sharp absorption edge disappeared as CuS content increases. The length of the single absorption edge of ZnS decreases rapidly and disappeared as more and more CuS is incorporated. It is a measure of content of CuS in the mixture. Compared to the intensity of 515 nm peak, intensity of the 470 nm peak of PL spectrum gets reduced and disappeared as the content of CuS is increased. Intensity ratio of the two peaks of the PL spectrum also gives information about the ratio of components in the mixture.

3.3 Electrical studies

Assuming that mobilities of holes and electron are independent of temperature the electrical conductivity of an intrinsic semiconductor is given by [19]

$\sigma=\sigma_0 T^{3/2} \exp(-E_g/2kT)$

Resistivity $\rho=\rho_0 T^{-3/2} \exp(E_g/2kT)$

Resistivity = Resistance*area/thickness

On using the same pellet area and thickness of the sample are constants.

Resistance(R) α Resistivity (ρ)

$R=R_0 T^{-3/2} \exp(E_g/2kT)$----------(1)

E_g is the intrinsic band gap energy and σ_0, ρ_0 and R_0 are constants, k and T are Boltzman constant and absolute temperature respectively.

The D.C electrical resistance of the pellet form of the samples were measured in the temperature range 310 K-485K. Fig (11a) shows the variation of resistance with temperature of zinc sulfide nanoparticles synthesized by solvothermal method. It consists of two regions. In the first region from 300K-420K it behaves as an insulator. There is no variation of resistance with temperature. Above 420K it has the semiconducting behaviour. Zinc sulfide behaves as like it needs some thermal energy to push it from the insulating state to the semiconducting state, may be because of its high band gap energy. The measured resistances at various temperatures were fitted to equation (1) using a nonlinear curve fitting c++ program developed using least square principle.

The best fit for the semiconducting region (430 K-485 K) was obtained for R0=1.42*10^9 and Eg=0.73eV. The measured resistances and the curve for

$$R=1.42*10^9*T^{-3/2}\exp(0.73/2kT)$$

for 430K-485K is shown in fig 11(b). Band gap energy 0.73 is in close agreement with the energy Ea (fig 6c)

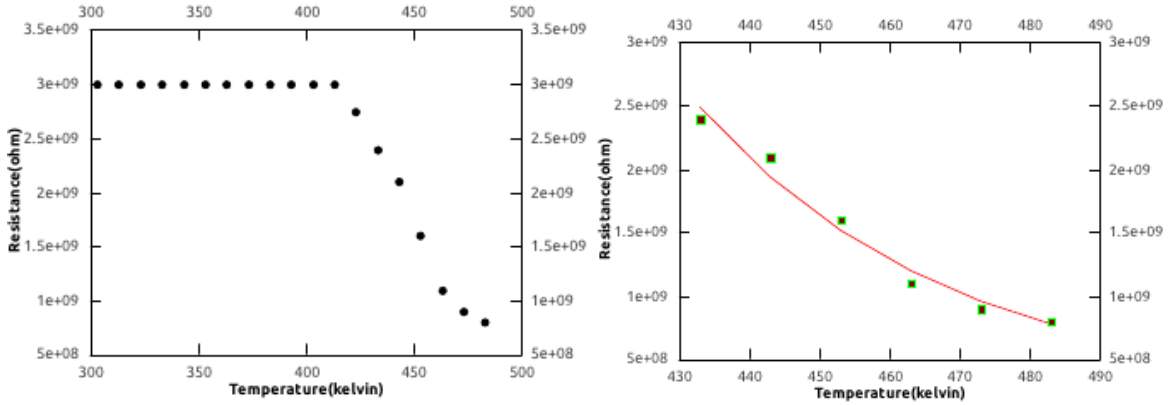

a b

Fig 11.a) Variation of resistance with temperature of ZnS nanoparticles, b) Experimental points and fitted curve for semiconducting region of ZnS nanoparticles

Fig (12) shows the variation of resistance with temperature of Zn.8Cu.2S nanoparticles synthesized by solvothermal method. There is no variation of resistance with temperature may be due to the insulating behaviour of zinc sulfide at lower temperature and at higher temperature due to the conducting behaviour of copper sulfide[12] and semi conducting behaviour of zinc sulfide . This sample can withstand high temperature (<500K) without any change in resistance.

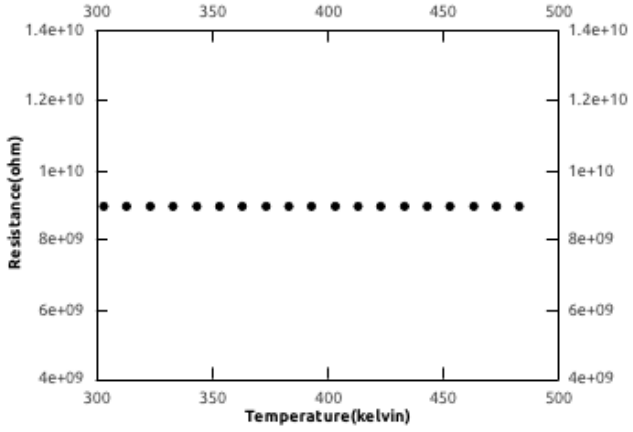

Fig. 12. Variation of resistance with temperature of $Zn_{.8}Cu_{.2}S$ nanoparticles

Fig (13a) shows the variation of resistance with temperature of $Zn_{.6}Cu_{.4}S$ nanoparticles synthesized by solvothermal method. It shows insulating behaviour up to 430K and then up to 470K due to large fluctuations resistance measurement becomes difficult indicating that the sample undergoes some phase transition. After heavy oscillation a jump in resistance from the order of 10^8 ohm to 10^3ohm was also observed at 470K. This sample can be used as a temperature

sensor. Above 470K the resistance decreases with increase in temperature showing the semiconducting behaviour.

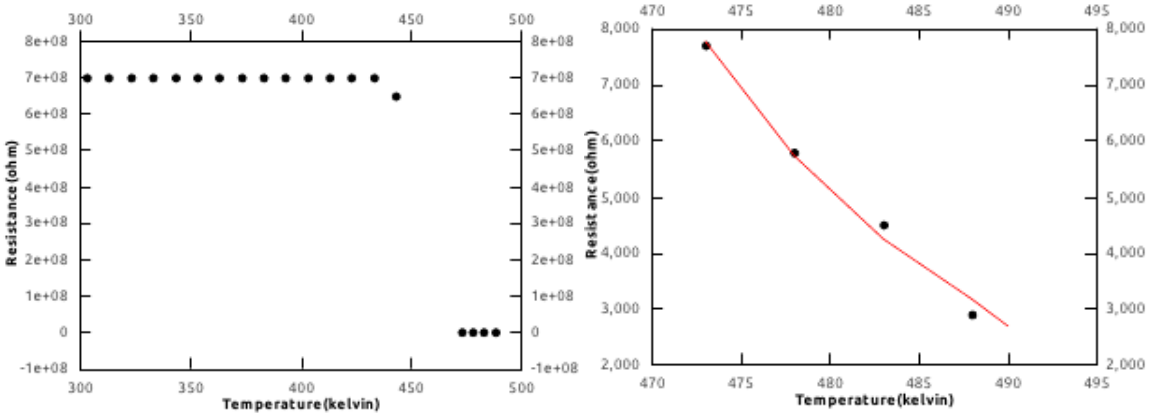

a b

Fig 13a) Variation of resistance with temperature of $Zn_{.6}Cu_{.4}S$ nanoparticles, b) Experimental points and fitted curve for Semiconducting region of $Zn_{.6}Cu_{.4}S$ nanoparticles

The measured resistances at various temperatures in the semiconducting region were fitted to equation(1).The best fit for the semiconducting region (470K-490K) was obtained for $R_0= 7.8*10^{-5}$and Eg=2.3eV. The measured resistances and the curve for

$$R=7.8*10^{-5}*T^{-3/2} \exp(2.3/2kT)$$

for 470K-490K is shown in fig (13b). The band gap energy 2.3 eV agrees with the first absorption edge (550nm) of the UV absorption spectrum of the same sample (fig 8a).

Fig (14a) shows the variation of resistance with temperature of $Zn_{.4}Cu_{.6}S$ nanoparticles. Up to 383K there is non uniform variation of resistance with temperature indicating that it is a region in the vicinity of phase transition. From 393K it shows the behaviour of a semiconductor. The semiconducting region can be fitted to band gap energy 1.9 eV (fig 14b) which agrees with the first absorption edge of the UV absorption spectrum of the same sample(fig 9a) .

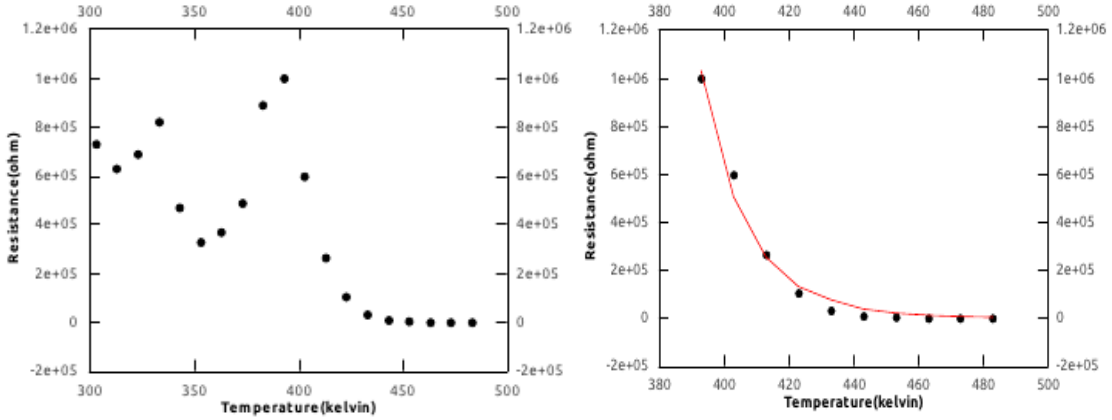

a b

Fig. 14.a) Variation of resistance with temperatureof $Zn_{.4}Cu_{.6}S$ nanoparticles, b) Experimental points and fitted curve for Semiconducting region of $Zn_{.4}Cu_{.6}S$ nanoparticles

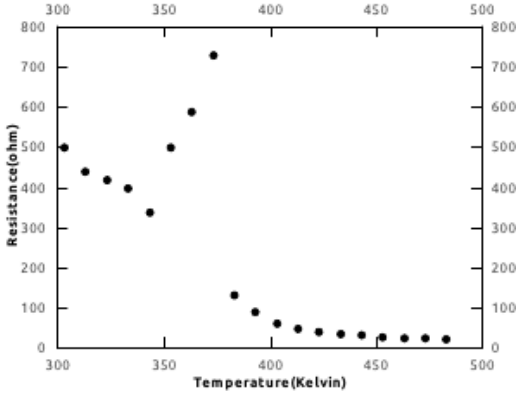

Fig. 15.a) Variation of resistance with temperature of Zn.2Cu.8S nanoparticles.

Fig (15a) shows the variation of resistance with temperature of $Zn_{.2}Cu_{.8}S$ nanoparticles . Up to 353K the sample behaves as a semiconductor. From 353K to 383K it shows the behaviour of a conductor like CuS [12] and above this temperature it again behaves as a semiconductor. The first semiconducting region can be fitted to band gap energy of 0.07eV (fig 15b) and the second semiconducting region can be fitted to band gap energy of 0.6eV (fig 15c).

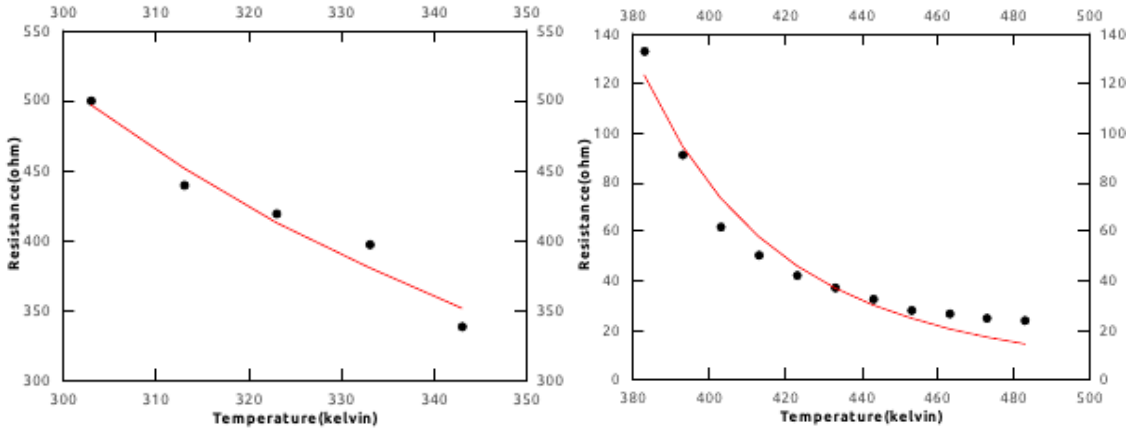

b c

Fig15. b) Experimental points and fitted curve for the first semiconducting region of $Zn_{.2}Cu_{.8}S$ nanoparticles, c) Experimental points and fitted curve for the second semiconducting region of $Zn_{.2}Cu_{.8}S$ nanoparticles

From electrical studies it is observed that samples of ZnS and $Zn_{.8}Cu_{.2}S$ are not undergoing any phase transition. From optical and electrical studies it is observed that nanoparticles with single sharp absorption edge do not undergo phase transition.

Table 6.3

Composition	Resistance(ohm)
$Zn_{.8}Cu_{.2}S$	9,00,00,00,000
$Zn_{.6}Cu_{.4}S$	70,00,00,000
$Zn_{.4}Cu_{.6}S$	6,30,000
$Zn_{.2}Cu_{.8}S$	440

The measured resistance at 313K for various composition using pellets of almost same size (circular pellet diameter = 13mm, distance between probes = 2mm) are tabulated in table3.Starting from $Zn_{.8}Cu_{.2}S$ nanoparticles resistances of the above samples rapidly decreases with the increase in the content of CuS.

4. Conclusion

$Zn_x Cu_{1-x} S$, x=1, .8, .6, .4 and .2 nanoparticles were synthesized by solvothermal method. The structure lattice parameter and size of the nanoparticles obtained from XRD pattern depend on the value of x. Very small size (2nm) of ZnS nanoparticles is also confirmed by SEM and AFM images. D.C electrical resistance measurement shows that upto 420K ZnS nanoparticles behave like an insulator and at higher temperatures it behaves as a semiconductor. PL emission spectrum of the ZnS nanoparticles shows one high intense peak at 475 nm and a low intense peak at 515nm. As the content of CuS increases the intensity of the high intense peak decreases and disappeared and the intensity of the low intense peak goes on increasing. Resistance measurement on $Zn_{.6}Cu_{.4}S$ nanoparticles shows a phase transition above 450K, $Zn_{.4}Cu_{.6}S$ above 380K and $Zn_{.2}Cu_{.8}S$ above 380K. It is also of interest that $Zn_{.6}Cu_{.4}S$ nanoparticles had a drastic switch from 10^8ohm to 10^3 ohm at 470K after heavy oscillation. The band gap energies obtained from resistance measurements agrees with that obtained from UV -VIS spectra. Starting from $Zn_{.8}Cu_{.2}S$ nanoparticles resistances of the above samples rapidly decreases with the increase in the content of CuS.

References

[1] N.R.Pawaskar, S.D Sathaye, M.M.Bhadhade, Mater.Res.Bull.**37**, 1539 (2002).
[2] X.Jiang, Y.Xie, J.Lu, Chem.Mater. **13**, 1213 (2001).
[3] S.Yamaga, A.Yoshikava, H.Kasai, J.Cryst.Growth, **86**,252 (1998).
[4] B.Elidrissi, M.Addou, M.Regragui, Mater.Chem.Phys .**68**, 175 (2001).
[5] C.Falcony, M.Garcia, A.Ortiz, J.Appl.Phys.**72**,1525 (1992).
[6] T.V.Prevenslik, J.Lumin.**87**,1210 (2000).
[7] C.N.Xu, T.Watannbe, M.Akiamma, Mater.Res.Bull**34**,1491 (1999).
[8] W.Tang, D.C.Cameron, Thin Solid films, **280**,221 (1996).
[9] W.Chen, Z.Wang, Z.Lin, Appl.Phys.Lett**70**, 1465 (1995).
[10] I.Puspitasari, T.P.Gujar, K.D.Jung, Mat.Sci.Eng.**140**, 199 (2007).
[11] Reijnen.L, Meester.B, Goossens.A, J.Chem.Vap.Deposition**9**, 15 (2003).
[12] R.Sheela Christy, J.ThampiThanka Kumaran, Journal of Non-Oxide Glasses, **6**, 13 (2014).
[13] Eunpyo Hong, Jung Hyeun, Nanoscale Science and Engineering Forum, Nov 5, 397a0 (2013).
[14] Shifu C, Mingsong J, J.NanosciNanotechnol**12**, 4898 (2012).
[15] A.L.Patterson, Phys.Rev.**56**,978 (1939).
[16] Nada K.Abbas, T.Khalid, In J.Electrochem.Sci, **8,**3049 (2013).
[17]H.V.Chung, P.T.Huy, J.Korean Physical Society, **52**,1562 (2008).
[18] W.Q.Peng, G.W.Cong, Optical Materials, **29**, 313 (2006).
[19] C.Kittel, Introduction to Solid State Physics, Wiley Eastern University, fifth ed. Pp231.